Journal of Molecular Catalysis A: Chemical 295 (2008) 1–9

Contents lists available at ScienceDirect

Journal of Molecular Catalysis A: Chemical

journal homepage: www.elsevier.com/locate/molcata

Porous hydrous zirconia supported 12-tungstophosphoric acid catalysts for liquid-phase esterification of 2-ethyl-1-hexanol

T. Rajkumar, G. Ranga Rao*

National Centre for Catalysis Research, Department of Chemistry, Indian Institute of Technology Madras, Chennai 600 036, India

ARTICLE INFO

Article history:
Received 7 May 2008
Received in revised form 21 July 2008
Accepted 16 August 2008
Available online 22 August 2008

Keywords:
Phosphotungstic acid
Esterification
2-Ethyl-1-hexanol
Acetic acid
Porous hydrous zirconia

ABSTRACT

12-Phosphotungstic acid supported on porous hydrous zirconia was prepared and characterized by N_2 adsorption isotherm, powder XRD, FTIR, ^{31}P MAS NMR, H_2-TPR, NH_3-TPD, SEM and TEM. It is found that the chemical interaction of Keggin anions with hydrous zirconia is different compared to the interaction with ZrO_2 and $Ce_{0.5}Zr_{0.5}O_2$ supports. The phosphotungstic acid clusters dispersed on porous hydrous zirconia did not show any split of IR bands at 1080 cm^{-1} (ν_{P-O}) and 983 cm^{-1} ($\nu_{W=O,ter}$) while those dispersed on ZrO_2 and $Ce_{0.5}Zr_{0.5}O_2$ showed a split in these two bands due to the lowering of symmetry of the central PO_4 tetrahedron and direct interaction of W=O_{ter} with oxide support. The dispersion of phosphotungstic acid on porous hydrous zirconia led to the growth of crystallites which showed catalytic activity for liquid-phase esterification of 2-ethyl-1-hexanol with acetic acid. Both conversion of 2-ethyl-1-hexanol and selectivity for 2-ethyl-1-hexyl acetate can be achieved at 100%.

1. Introduction

Heteropoly acids (HPAs) are polyprotic oxides that are used as solid acids and catalysts for homogeneous selective oxidation [1,2] and heterogeneous esterification reactions [3–12]. These catalysts are environmentally benign and very effective for oxidation reactions with H_2O_2 and O_2 [1,2]. A number of attempts have been made to develop efficient heterogeneous catalysts with heteropoly acids dispersed on supports such as hydrous zirconia [5], $Ce_{0.5}Zr_{0.5}O_2$ [13], SiO_2 [14], intercalated anion-exchange materials and resins [4,11], surface modified mesoporous materials such as MCM-41, SBA-15 [9,15–17] and anchored-SiO_2 surfaces [18]. Dispersion of heteropoly acids is important for catalytic applications because of the low surface area of unsupported HPA (~10 m^2/g). The chemical interaction and bonding, molecular dispersion, thermal stability of Keggin molecular species and their catalytic activity depend on the nature of the solid support (surface area, porosity, acidic or neutral and sorption property) and HPA loading. Literature search shows that there are several factors which are taken into account for heterogenization of polyoxometalates. The main factors considered in heterogenization of heteropoly acids are electrostatic interaction with supports, porous nature of supports, ionic interactions to form solid ionic materials with polyanions, insertion of Keggin anions in hydrotalcite-like anion exchange materials, immobilization of heteropolyanions as molecular species on chemically modified silicate surfaces. The dispersed HPA catalysts have been studied for their catalytic activity towards acid catalysed reactions such as esterification, alkylation, acylation, isopropanol dehydration, MTBE synthesis and *tert*-butylation reactions [5,6,11,13,16–21].

Hydrous zirconia (HZ) is a compatible support with heteropoly acids [5,12,18–21]. Phosphotungstic acid (PWA) supported on hydrous zirconia is reported as a promising catalyst for the esterification of canola oil with methanol exhibiting ~77% yield [21]. Generally, zirconium hydroxide ($Zr(OH)_{4n}H_2O$) is regarded as hydrous zirconia ($ZrO_{2n}H_2O$), a precursor from which ultrafine zirconia powder is obtained by calcination. There are some important structural differences observed between these two phases. Zirconium hydroxide is a tetramer, $[Zr_4(\mu\text{–}OH)_8(OH)_8(H_2O)_8]xH_2O$, in which the Zr atoms are linked by a pair of hydroxo bridges. The bonding pattern in hydrous zirconia is similar to that of zirconium hydroxide except that Zr atoms are linked by an oxide bond, not a pair of hydroxo bridges [22]. Both materials contain coordinated water molecules. Because of the Zr–O–Zr linkages present in hydrous zirconia, it retains less number of bridging and non-bridging hydroxo groups when compared to zirconium hydroxide. Since the bridging hydroxo groups can behave like Brønsted acid sites, hydrous zirconia is expected to show less Brønsted acidity than zirconium hydroxide. The Zr–O–Zr linkages, bridging and non-bridging hydroxyl groups provide hydrous zirconia the ability to

* Corresponding author. Tel.: +91 44 2257 4226; fax: +91 44 2257 4202.
E-mail address: grrao@iitm.ac.in (G. Ranga Rao).

1381-1169/$ – see front matter © 2008 Elsevier B.V. All rights reserved.
doi:10.1016/j.molcata.2008.08.008

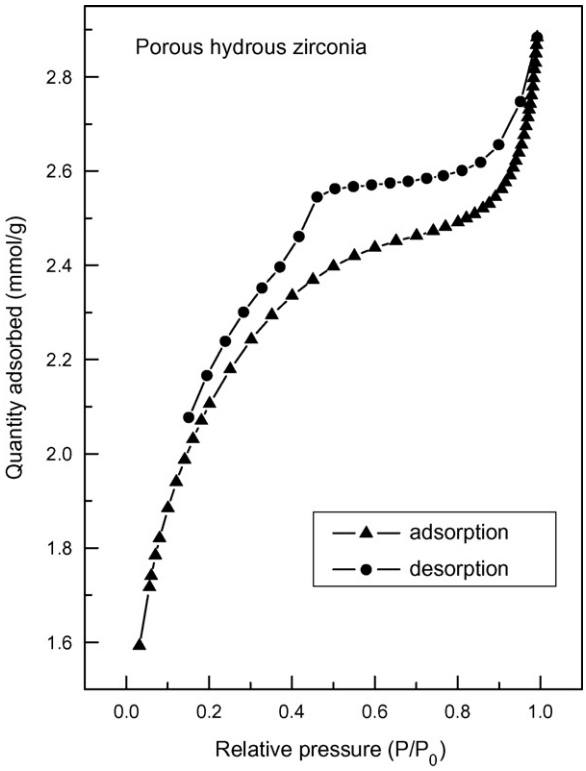

Fig. 1. N_2 adsorption–desorption isotherm of hydrous zirconia (HZ).

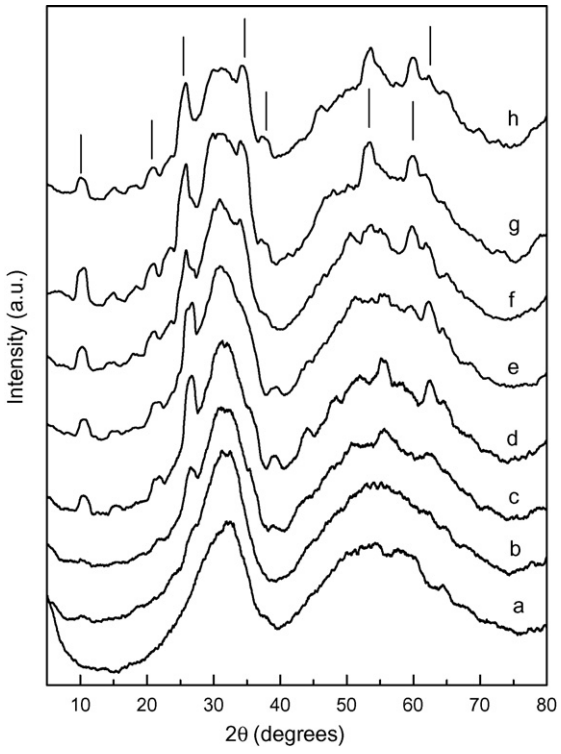

Fig. 2. XRD pattern of (a) HZ, (b)–(h): 10 wt%, 15 wt%, 20 wt%, 25 wt%, 30 wt%, 35 wt%, and 40 wt% PWA dispersed on hydrous zirconia.

interact with and stabilize the dispersed catalytic species such as Keggin ions.

The chemical interaction and catalytic ability of strong Brønsted type 12-tungstophosphoric acid supported on hydrous zirconia is a subject of numerous recent investigations which demonstrate the versatility of this unique solid acid catalyst for *tert*-butylation of *m*-cresol [20], esterification and transesterification reactions [5,21], synthesis of linear alkyl benzenes [23], and oxidative bromination of phenol [24]. The significant features of this catalytic system include the stability of Keggin species on hydrous zirconia [5,25], monoclinic to tetragonal phase transition of zirconia in the presence of PWA [23], availability of Brønsted and Lewis acidity [16], and generation of Lewis acid sites by chemical interaction between PWA and surface hydroxyl groups of zirconia [25]. Catalyst recycling and eco-friendly nature are the other important features of this solid acid catalyst. In an effort to design heterogenized heteropoly acid catalysts on compatible and non-conventional oxide supports such as $Ce_xZr_{1-x}O_2$ [13], we have undertaken a detailed study on the porous hydrous zirconia supported 12-tungstophosphoric acid and carried out esterification of 2-ethyl-1-hexanol with acetic acid. It is found that the nature of interaction of Keggin anions with porous hydrous zirconia is different compared to the interaction with ZrO_2 and $Ce_xZr_{1-x}O_2$ solid solutions.

Table 1
Surface area and pore volume of PWA loaded hydrous zirconia catalysts

Catalyst	SA (BET) ($m^2\ g^{-1}$)	Pore volume ($cm^3\ g^{-1}$)
Hydrous zirconia	157	0.110
10 wt% PWA/HZ	149	0.099
15 wt% PWA/HZ	144	0.099
20 wt% PWA/HZ	138	0.097
25 wt% PWA/HZ	131	0.087
30 wt% PWA/HZ	118	0.083
35 wt% PWA/HZ	104	0.068
40 wt% PWA/HZ	95	0.063

2. Experimental

2.1. Preparation of PWA/porous hydrous zirconia

Zirconium hydroxide gel was prepared from zirconium oxychloride aqueous solution (S.D. Fine Chem Ltd.) by adding drop wise ammonium hydroxide solution (SRL) up to pH 9.5. The hydrogel was refluxed at room temperature for 24 h, then filtered and washed with deionized water and dried in an oven at 110 °C for 24 h. The sample could not be dissolved but suspended in nitric acid which confirmed the formation of hydrous zirconia [22]. The PWA/hydrous zirconia catalysts were prepared by wet impregnation method. The PWA dispersed in ethanol solution was added drop wise to the support by continuous stirring at room temperature. The samples were dried at 100 °C overnight and calcined at 300 °C for 5 h in air. For comparative studies, ZrO_2 was prepared by combustion method, and $Ce_xZr_{1-x}O_2$ samples were prepared by sol–gel combustion method. 20 wt% of PWA was impregnated on these supports by the same method discussed above.

2.2. Characterization of catalysts

All samples were analysed by X-ray diffraction employing Shimadzu XD-D1 diffractometer using Cu Kα radiation (λ = 1.5418 Å). The surface area and pore volume of powder samples were obtained from Micromerticis ASAP 2020 machine. The KBr pellet method was used to record IR spectra of samples on a PerkinElmer IR spectrometer with a resolution of 4 cm^{-1} in the range of 450–4000 cm^{-1}. The ^{31}P MAS NMR spectra of bulk PWA and dispersed PWA catalysts were recorded using Bruker Avance 400 spectrometer at resonance frequency of 161.97 MHz for ^{31}P nuclei with Bruker CP MAS probe and the chemical shifts are reported in ppm (δ) relative to external 85 wt% H_3PO_4. The ^{31}P MAS NMR spectra were recorded with a sample spinning rate of 8 kHz, and the delay between two pulses was

Table 2
IR and ^{31}P MAS NMR spectral data of supported PWA catalysts

Catalyst	^{31}P MAS NMR (ppm)	Wavenumber (cm^{-1})			
		P–O	W=O_{ter}	W–O_{corner}–W	W–O_{edge}–W
$H_3PW_{12}O_{40}\cdot nH_2O$	−15.1	1080	987	890	810
10 wt% PWA/HZ	−14.8	1080	984	890	810
15 wt% PWA/HZ	−14.8	1080	983	890	810
20 wt% PWA/HZ	−13.6, −15.1	1080	984	890	810
25 wt% PWA/HZ	−13.7, −14.8	1080	984	890	810
30 wt% PWA/HZ	−13.6, −15.0	1080	984	890	810
35 wt% PWA/HZ	−13.6, −15.0	1080	984	890	810
40 wt% PWA/HZ	−13.5, −14.9	1080	984	890	810
20 wt% PWA/ZrO_2	−14.2, −15.0, −15.6	1080, 1058	984, 962	890	810
20 wt% PWA/$Ce_{0.5}Zr_{0.5}O_2$	−14.0, −15.0, −16.1	1080, 1056	982, 964	892	816

2 s for relaxation of the ^{31}P nuclei. Scanning electron microscopy (SEM) pictures were taken using FEI Quanta 200 microscope. The sample powders were deposited on a carbon tape before mounting on a sample holder. The TEM images of the samples were taken using JEOL JEM-3010 transmission electron microscope. The material was dispersed in acetone and deposited onto a 200-mesh size carbon coated copper grid. The TEM images were recorded with a slow-scan CCD camera.

The temperature programmed reduction (TPR) of samples was carried out on Micromeritics Chemisorb 2750 instrument. TPR was carried out from room temperature to 900 °C in 5% H_2 in Ar at a flow rate of 20 ml min^{-1}. Linear heating of 10 °C min^{-1} was employed and the water produced by reduction was trapped in slurry of isopropyl alcohol cooled by liquid nitrogen.

The acidity of the catalysts was measured by temperature programmed desorption of NH_3 (NH_3-TPD) using Micromeritics Chemisorb 2750 instrument. It was carried out after ~0.02 g of the catalyst sample was pre-treated at 300 °C in He (20 cm^3 min^{-1}) for 1 h. The temperature was then decreased to 100 °C under He flow, and NH_3 was adsorbed by exposing samples to a stream of 9.34% NH_3 in He for 30 min at the same temperature. It was then flushed with He gas for 60 min at 100 °C to remove physisorbed NH_3. The sample was cooled to room temperature in He flow. The desorption of NH_3 was carried out in He flow (20 cm^3 min^{-1}) by increasing temperature to 750 °C at a rate of 10 °C min^{-1} and measuring NH_3 desorption using a TCD detector.

2.3. Esterification reaction

Esterification reactions were carried out in a stainless steel autoclave (10 ml) in the temperature range 60–100 °C under autogenous pressure. Calculated amounts of reaction mixture (2-ethyl-1-hexanol and acetic acid) were taken into an autoclave and 100 mg of freshly activated catalyst was added. Activation of the catalyst was done by calcination at 300 °C in air for 5 h. The autoclave temperature was then raised to 60 °C, 80 °C and 100 °C as required and maintained at the desired temperature during the reaction period. After the reaction, the autoclave was cooled to room temperature,

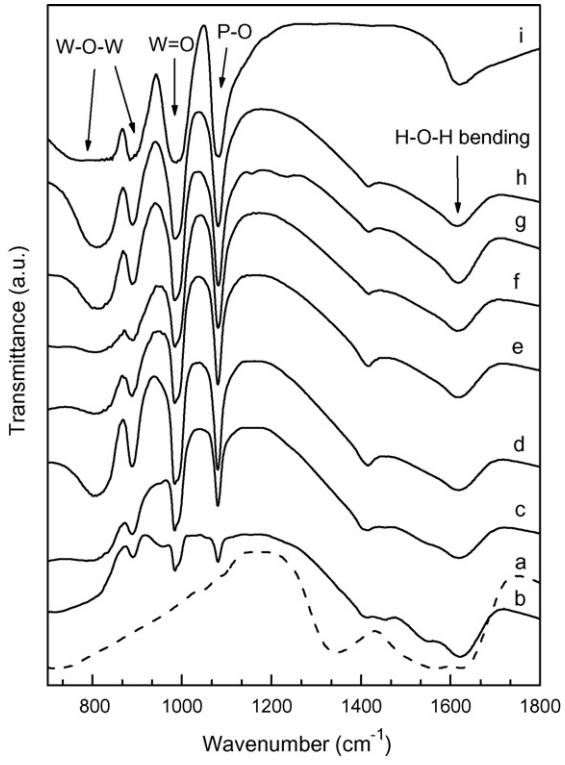

Fig. 3. FTIR spectra of (a) HZ, (b)–(h): 10 wt%, 15 wt%, 20 wt%, 25 wt%, 30 wt%, 35 wt%, and 40 wt% PWA dispersed on HZ, and (i) pure PWA.

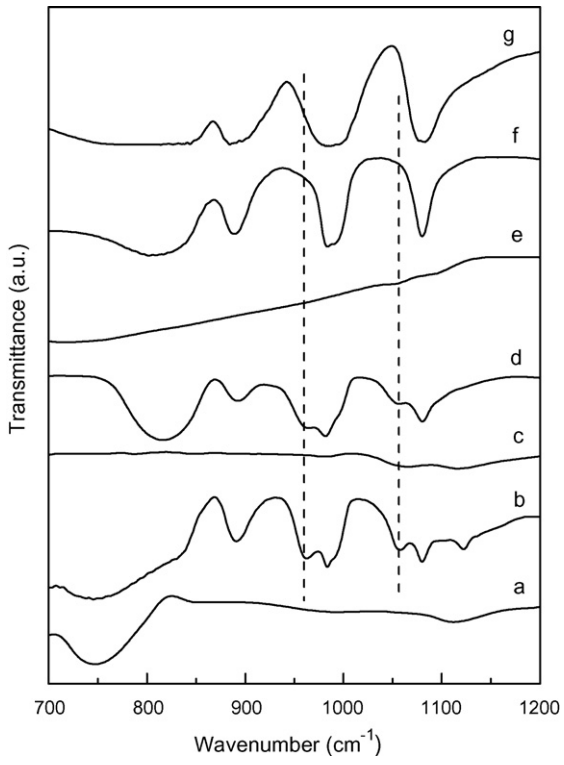

Fig. 4. FTIR spectra of (a) ZrO_2, (b) 20 wt% PWA/ZrO_2, (c) $Ce_{0.5}Zr_{0.5}O_2$, (d) 20 wt% PWA/$Ce_{0.5}Zr_{0.5}O_2$, (e) HZ, (f) 20 wt% PWA/HZ and (g) pure PWA.

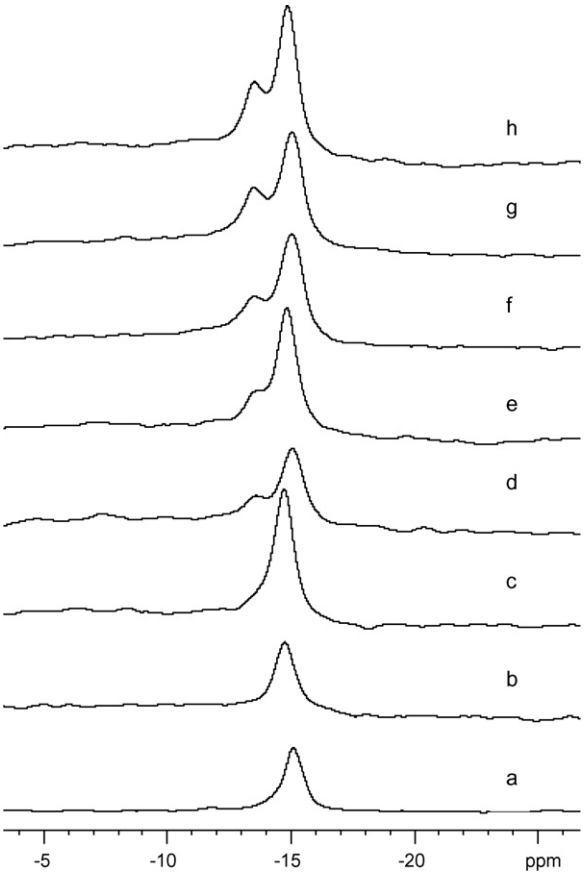

Fig. 5. ^{31}P MAS NMR spectra of (a) pure PWA, (b)–(h): 10 wt%, 15 wt%, 20 wt%, 25 wt%, 30 wt%, 35 wt%, and 40 wt% PWA dispersed on HZ.

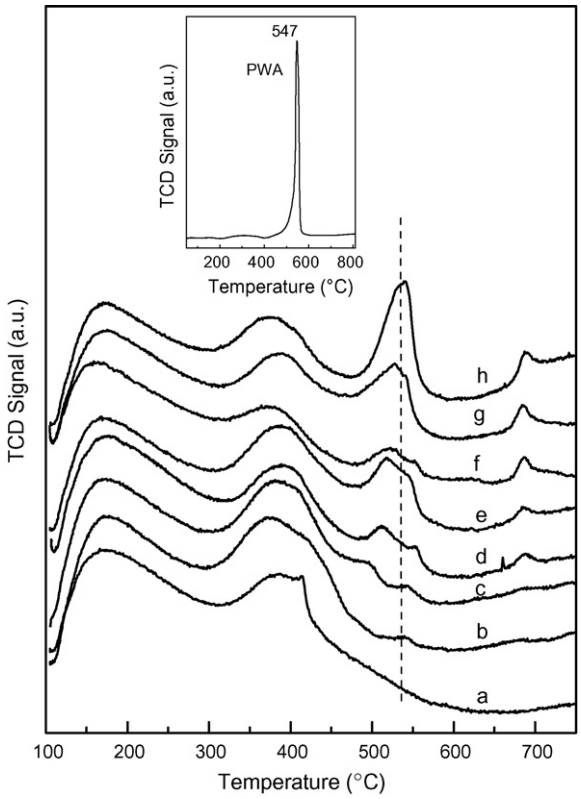

Fig. 6. NH_3-TPD of (a) HZ, (b)–(h): 10 wt%, 15 wt%, 20 wt%, 25 wt%, 30 wt%, 35 wt%, and 40 wt% PWA dispersed on HZ. Inset is the TPD of pure PWA.

the reaction mixture was collected from the autoclave and the catalyst was removed by filtration. The effect of reaction time, molar ratios of the reactants, and amount of catalyst required on alcohol conversion and product selectivity were studied. Conversions are reported on weight basis in the text. Analysis of the products was carried out by a gas chromatograph (AMIL–Nucon 5765) using a HP-1 capillary column (cross-linked methyl silicone gum, 25 m × 0.2 mm × 0.33 μm film thickness) and a flame ionization detector.

3. Results and discussion

3.1. Porosity analysis

Porosity in hydrous zirconium oxide originates from the preparation conditions which directly influence its morphology, microstructure and thermal stability [26–30]. Fig. 1 shows the typical nitrogen adsorption–desorption isotherm measured on hydrous zirconia samples prepared in this study. The hysteresis loop indicates well-developed porous network of the material with capillary condensation taking place in mesopores. Adsorption hysteresis indicates slit-like pores resembling H4 type loop which does not close even at lower limit of $P/P_0 = 0.42$. Hydrous zirconia shows variety of isotherms including H2 type hysteresis and wide distribution of pore diameters (~20 Å to >100 Å) depending on the digestion treatment and pH [27,29,30]. The porous hydrous zirconia described here is further used for preparing supported phosphotungstic acid catalysts in this study. The surface area and pore volume data for porous hydrous zirconia and PWA loaded catalyst samples are presented in Table 1. As expected, the surface area and pore volume values are consistently decreasing with PWA loading on porous hydrous zirconia.

3.2. Powder X-ray diffraction analysis

Fig. 2 shows the powder XRD of hydrous zirconia and 10–40 wt% PWA loading on hydrous zirconia support. Hydrous zirconia shows two very wide diffraction structures peaked at ~32° and ~54° which are typical of amorphous nature of the material [24,25]. When PWA is loaded the broad XRD structures of hydrous zirconia are not affected indicating that crystallization of amorphous support does not occurs at calcination temperatures <350 °C. Higher calcination temperatures are required for hydrous zirconia to yield mixture of tetragonal and monoclinic phases [23,31]. The weak diffraction peaks at 10.2°, 20.7°, 25.7°, 34.3°, 37.6°, 53.1°, 59.8° and 62.1° superimposed on broad PXRD structure are due to the growth of PWA crystallites dispersed on amorphous hydrous zirconia. The growth of PWA crystallites has been previously shown to occur on silica support by López-Salinas et al. [25] and Kuang et al.

Table 3
H_2-TPR and NH_3-TPD data for PWA/HZ catalysts

Catalyst	NH_3-TPD peak Temperature (°C)	H_2-TPR peak Temperature (°C)
HZ	170, 390	632
10 wt% PWA/HZ	171, 370, 687	462, 593, 768
15 wt% PWA/HZ	169, 381, 687	630
20 wt% PWA/HZ	176, 389, 511, 687	652
25 wt% PWA/HZ	170, 389, 518, 687	658
30 wt% PWA/HZ	159, 375, 523, 687	698
35 wt% PWA/HZ	175, 384, 528, 687	690, ~843
40 wt% PWA/HZ	170, 375, 539, 687	708, 846
PWA	547	450, 557, >640

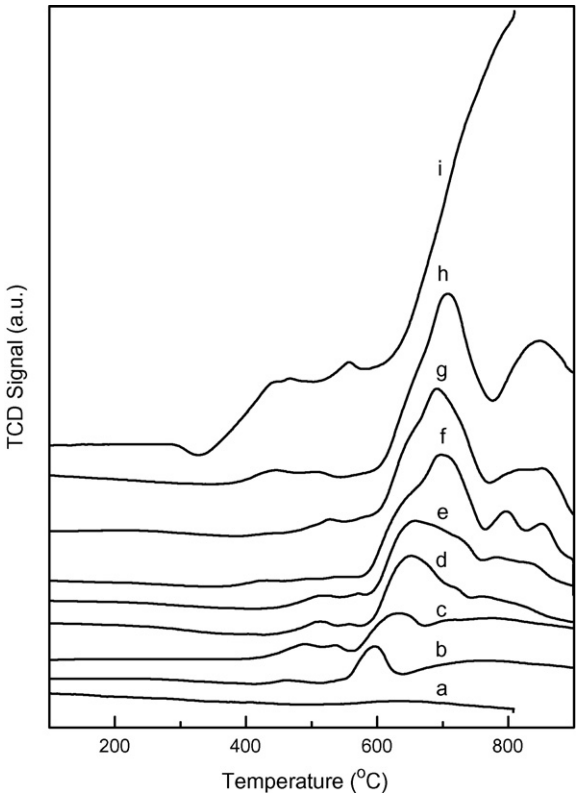

Fig. 7. H_2-TPR of (a) HZ, (b)–(h): 10 wt%, 15 wt%, 20 wt%, 25 wt%, 30 wt%, 35 wt%, and 40 wt% PWA dispersed on HZ and (i) pure PWA.

[32]. However, due to stronger interaction, molecular dispersion of PWA appears to be favourable on ZrO_2 [23–25,33] and $Ce_xZr_{1-x}O_2$ supports [13].

3.3. FTIR analysis

The interaction of PWA species with hydrous zirconia has been examined in the IR fingerprint region of 700–1200 cm^{-1}. The spectra in Fig. 3 show vibrational bands pertaining to PWA developing at 810 cm^{-1} (W–O_e–W stretch), 890 cm^{-1} (W–O_c–W stretch), 984 cm^{-1} (W=O terminal) and 1080 cm^{-1} (P–O stretch) as a function of PWA loading on hydrous zirconia. In our earlier study [13], we reported that the bands at 1080 cm^{-1} and 984 cm^{-1} are split due to the interaction of the W=O terminal bond of the Keggin unit with Lewis acid centers on the $Ce_{0.5}Zr_{0.5}O_2$ solid solution. The present study further shows that the nature of interaction of the Keggin units is different with $Ce_{0.5}Zr_{0.5}O_2$ solid solution and hydrous zirconia. To clarify this point, the IR spectra of PWA dispersed on ZrO_2, $Ce_{0.5}Zr_{0.5}O_2$ and hydrous zirconia are shown in Fig. 4. The IR spectra clearly display the split in 1080 cm^{-1} and 983 cm^{-1} bands in the case of ZrO_2 and $Ce_{0.5}Zr_{0.5}O_2$ but not for hydrous zirconia. The results of IR and ^{31}P MAS NMR analysis of the supported $H_3PW_{12}O_{40}$ composite samples are summarized in Table 2. The previous IR studies of López-Salinas et al. [25], Qu et al. [31] and Jiang et al. [34] on zirconia supported $H_3PW_{12}O_{40}$ composites showed prominent shifts/splits in the IR stretching bands of P–O bond, W=O_{ter} bond and W–$O_{e/c}$–W bonds. These shifts/splits are generally noted for uncalcined composite samples, and ascribed to the interaction of Keggin units with zirconia support and the symmetry decrease of the central PO_4 tetrahedron. The red-shift in the ν_{as} vibration of W=O_{ter} bond has been interpreted due to the weakening of the anion cohesion [25] or the interaction of the terminal oxygen with the cationic Lewis sites as reported on $Ce_{0.5}Zr_{0.5}O_2$ solid solution [13]. There is also an effect of solvent used in impregnating $H_3PW_{12}O_{40}$ on the support [35] and final calcination temperature [25]. In the present study, the composite catalyst samples prepared by impregnation with ethanol solution of $H_3PW_{12}O_{40}$ on hydrous zirconia do not show the shift/split in the characteristic IR bands while impregnation with aqueous solution of $H_3PW_{12}O_{40}$ on zirconia and $Ce_{0.5}Zr_{0.5}O_2$ solid solution leads to split in the IR bands (Figs. 3 and 4 and Table 2). This suggests that aqueous impregnation of $H_3PW_{12}O_{40}$ appears to be a key factor for stronger interaction facilitating molecular dispersion of Keggin units on oxide supports at lower loadings. The surface hydroxyl groups on hydrated zirconia, Zr–OH, play a role in stabilizing Keggin species by acid–base type interaction [25].

3.4. ^{31}P MAS NMR analysis

^{31}P MAS NMR technique is extremely sensitive to ^{31}P local electron density and water of hydration in the bulk as well as dispersed phosphotungstic acid crystallites on oxide supports. It is a tool often used to discern various types of surface Keggin species present in heteropoly acid catalysts. Fig. 5 displays the ^{31}P MAS NMR spectra for bulk PWA and PWA/HZ samples. The bulk PWA shows a sharp signal at −15 ppm characteristic of phosphorus in the central position of the Keggin unit [13,32]. One resonance peak at −14.8 ppm is observed for 10 wt% and 15 wt% PWA loaded on porous hydrous zirconia support. This peak is essentially due to the bulk-type PWA and its intensity grows with PWA loading. It is assigned to the Keggin anions which are structurally intact on hydrous zirconia. As PWA loading is increased from 20 wt% to 40 wt%, an intense resonance peak is observed in the range of −14.8 ppm to −15.1 ppm with a small shoulder around −13.6 ppm. The former is due to the intact Keggin anion crystallites while the shoulder is attributed to the distorted intact Keggin species interacting with Zr–OH groups of the hydrous zirconia. Two types of Keggin species, interfacial molecular and bulk, have been identified previously in the dispersed layers of phosphotungstic acid on ZrO_2 [25,34,36], $Ce_xZr_{1-x}O_2$ [13], SiO_2 [14,35,36] and SiMCM-41 [37] supports, and their relative amounts and activity depends on loading. This study reveals that Zr–OH groups present in the porous hydrous zirconia are involved in stabilizing Keggin ions by forming surface ion pairs, such as $(\equiv Zr\text{–}OH_2)_n^+(H_{3-n}PW_{12}O_{40})^{n-3}$ on hydrated ZrO_2 [25,36] and $(\equiv SiOH_2)^+(H_2PW_{12}O_{40})^-$ on SiO_2 [14,35].

3.5. NH_3-TPD analysis

The acidic properties of heteropoly acid catalysts can be studied by temperature programmed desorption of NH_3 and IR of adsorbed pyridine. NH_3-TPD profiles of bulk PWA (inset), hydrous zirconia and hydrous zirconia supported PWA are shown in Fig. 6. Two broad desorption peaks appeared at 170 °C and 380 °C in the spectrum of uucalcined porous hydrous zirconia. In addition to these two desorption peaks, two new peaks have appeared at 533 °C and 686 °C from PWA loaded hydrous zirconia samples. The bridging and non-bridging hydroxyl groups present in hydrous zirconia can act as either basic sites or as acidic sites. Therefore, the two peaks at 170 °C and 380 °C are attributed to desorption of weakly adsorbed basic molecule from Brønsted acidic sites essentially arising from non-bridging and bridging hrdroxo groups, respectively, of hydrous zirconia. These acidic sites continue to exit even after PWA loadings but the total number appeared to have decreased above 15 wt% loading. The strong desorption peak appeared at 533 °C, which has grown out of two smaller split peaks as a function of PWA loading, could be ascribed to desorp-

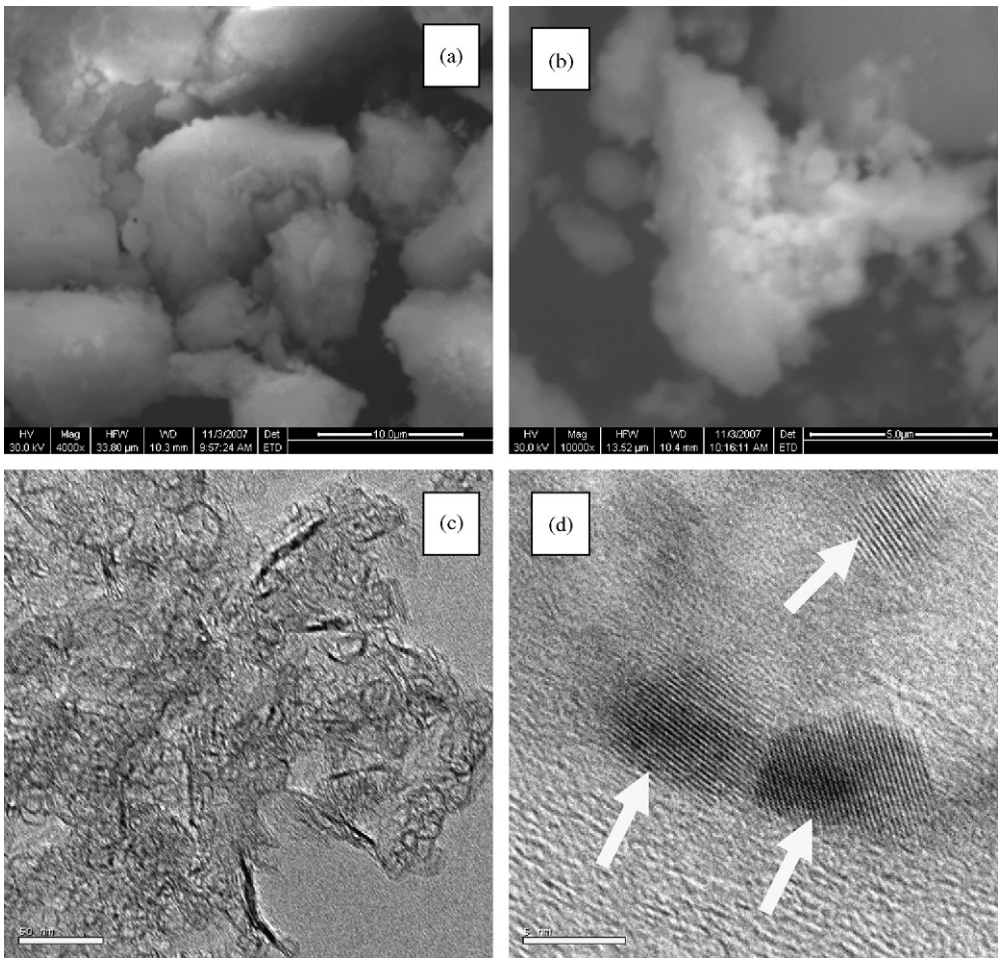

Fig. 8. SEM images of (a) HZ (10 μm) and (b) 35 wt% PWA dispersed on HZ (5 μm); TEM images of (c) HZ (50 nm) and (d) 35 wt% PWA dispersed on HZ (5 nm). Arrows show the PWA crystallites on HZ support.

tion of the chemisorbed NH_3 and N_2 from PWA accompanied by its decomposition above 500 °C [13,38]. Koyano et al. [39] reported NH_3-TPD spectrum of PWA with desorption peak at 577 °C and showed that it is accompanied by the formation of N_2 as per the reaction, $2NH_3 + 3O(\text{polyanion}) \rightarrow N_2 + 3H_2O$. The remaining peak at 686 °C, which becomes prominent as function of PWA loading, can be attributed to base desorption from the decomposed product WO_3 [13]. In summary the PWA loaded hydrous zirconia contains at least three different acidic sites originated from (i) hydroxyl groups of hydrous zirconia and (ii) strong and uniform acidic sites from dispersed PWA (Table 3).

3.6. H_2-TPR analysis

It is known that the H_2-TPR technique provides valuable information about the reducibility of individual species, making it a useful tool to study heteropoly acid catalytic materials. The thermal reduction behaviour of PWA loaded hydrous zirconia catalysts is displayed in Fig. 7. The TPR of porous hydrous zirconia does not show significant H_2 consumption (Fig. 7a). The dispersed PWA on porous hydrous zirconia shows distinct reduction behaviour above 400 °C which gradually changes to bulk type reduction behaviour with increased PWA loading. There is a broad weak TPR peak in the region 400–550 °C due to the deprotonation of acid with concurrent non-reductive loss of lattice oxygen [13,40]. The major reduction occurred at 550–775 °C, and the reduction maximum at 595 °C for 10 wt% lading shifts to 707 °C for 40 wt% loading of PWA on hydrous zirconia. This strong reduction peak appears at a temperature higher than PWA decomposition temperature. The PWA hydrate begins to decompose at 470 °C by loosing 1.5 H_2O and its thermal decomposition is complete above 610 °C [13,41]. The shift of the peak maximum to higher temperatures in Fig. 7 suggests that the dispersed PWA decomposition on hrdrous zirconia support depends on the amount loaded and crystallite size. The reduction maximum gradually shifts toward the bulk reduction temperature above 700 °C (Table 3). Therefore the reduction region 550–775 °C is due to the decomposition and extensive reduction of Keggin units and constituent oxides. The reduction above 750 °C is due to the reduction of decomposition product WO_3.

3.7. SEM and TEM analyses

Powder XRD has shown the growth of crystallites of PWA at higher loadings on hydrous zirconia. In order to check this point we have carried out microscopy study. Fig. 8 displays the SEM and TEM images of hydrous zirconia and 35 wt% PWA dispersed on hydrous zirconia catalysts. The SEM (Fig. 8a) and TEM images (Fig. 8c) of hydrous zirconia exhibit clearly its amorphous and hydrous nature. After loading 35 wt% PWA and calcining at 300 °C, the amorphous nature of the support is retained and dispersed PWA crystallites of size ~7 nm can be seen in Fig. 8d. It is therefore evident that growth of small crystallites occurs at higher loadings of PWA on amorphous hydrous zirconia support.

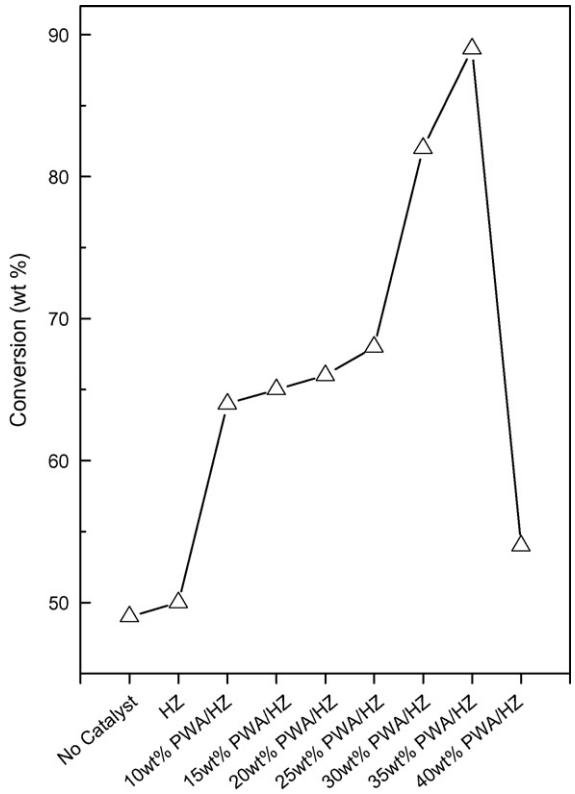

Fig. 9. Effect of PWA loading on the esterification of 2-ethyl-1-hexanol with acetic acid at 100 °C in 4 h (molar ratio of alcohol/acid = 1:2, catalyst 0.1 g).

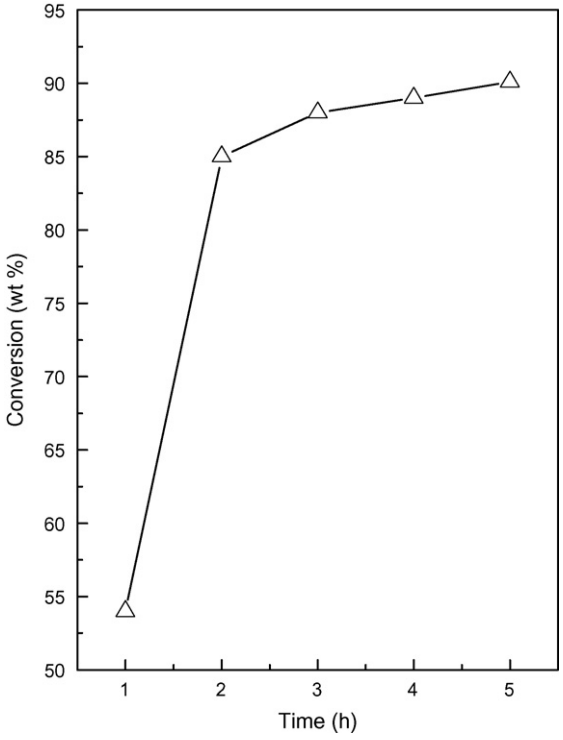

Fig. 10. wt% conversion of 2-ethyl-1-hexanol with different reaction times on 35 wt% PWA/HZ catalyst at 100 °C (molar ratio of alcohol/acid = 1:2, catalyst 0.1 g).

3.8. Esterification reaction

Esterification reactions using heteropoly acids dispersed on various supports have been investigated extensively [5–7,11,12,19,21,42,43]. However, esterification of acetic acid with 2-ethyl-1-hexanol has commercial application to extract dilute acetic acid as ester in excess water, and the reaction has been studied in the presence of sulphated zirconia [42], MCM-41 [43], and acidic cation exchanger (Amberlyst 15) [44]. In the present study, the reaction is carried out in liquid-phase on hydrous zirconia supported PWA catalysts by using excess acetic acid as a reactant. This is one of the commonest approaches to shift the chemical equilibrium towards product side [5,7,43], the other being continuous removal of the water formed [19].

3.8.1. Influence of PWA loading

The influence of PWA loading on the conversion of 2-ethyl-1-hexanol has been studied in autogenous pressure using 0.10 g of catalyst and reactant ratio of 1:2 (alcohol/acid) for a period of 4 h at 100 °C. The results are shown in Fig. 9. The esterification reaction shows about 49% conversion without any catalyst and no significant change in conversion has occurred in the presence of hydrous zirconia catalyst. However, the reaction proceeds efficiently over PWA loaded hydrous zirconia catalysts and conversion reaches 89% at 35 wt% PWA loading. The increase in conversion with PWA loading is generally attributed to the availability of catalytically active Brønsted acid sites from PWA crystallites of optimum size ~8 nm (TEM picture in Fig. 8d). There is a possibility for the synergetic participation of Brønsted acid sites of hydrous zirconia and PWA in esterification reaction. The selectivity is 100% towards 2-ethyl-1-hexyl acetate irrespective of PWA loading. The reaction has been further studied to optimize reaction time, catalyst concentration, reaction temperature, mole ratio of the reactants on 35 wt% PWA/HZ catalyst.

3.8.2. Influence of reaction time

The effect of reaction time on the conversion of 2-ethyl-1-hexanol over 35 wt% PWA/HZ is shown in Fig. 10. The reaction has been carried out on 0.10 g catalyst using alcohol/acid ratio 1:2 at 100 °C. The initial conversion of 2-ethyl-1-hexanol during 1 h reaction time is 54% and it has increased to a maximum of 90.1% in 5 h of reaction. The selectivity towards 2-ethyl-1-hexyl acetate is 100% in all cases.

3.8.3. Effect of catalyst weight

The reaction has been carried out by varying the amount of 35 wt% PWA/HZ catalysts between 0.05 g and 0.25 g keeping alcohol/acid ratio fixed at 1:2 for 5 h at 100 °C before product analysis. The effect of the amount of catalyst on the 2-ethyl-1-hexanol conversion is shown in Fig. 11. The increase in catalyst weight from 0.05 g to 0.10 g increases the conversion of 2-ethyl-1-hexanol from 70.3% to 90.1%. Further increase in catalyst weight has no effect on conversion levels. This reaction behaviour of increased conversion with increased catalyst weight can be attributed to an increase in the availability and number of catalytically active sites to the reactant molecules. Esterification reaction can be initiated on the catalyst by a proton donation to adsorbed acetic acid molecule and the protonated acid molecule is accessible for a nucleophilic attack by the hydroxyl group of 2-ethyl-1-hexanol. The reaction can take place on the catalyst surface continuously with water elimination.

3.8.4. Influence of temperature

In order to determine the effect of reaction temperature, esterification reaction is performed at 60 °C, 80 °C and 100 °C using 0.10 g of 35 wt% PWA/HZ catalyst and alcohol/acid ratio of 1:2 for 5 h. The conversion of 2-ethyl-1-hexanol as a function of temperature

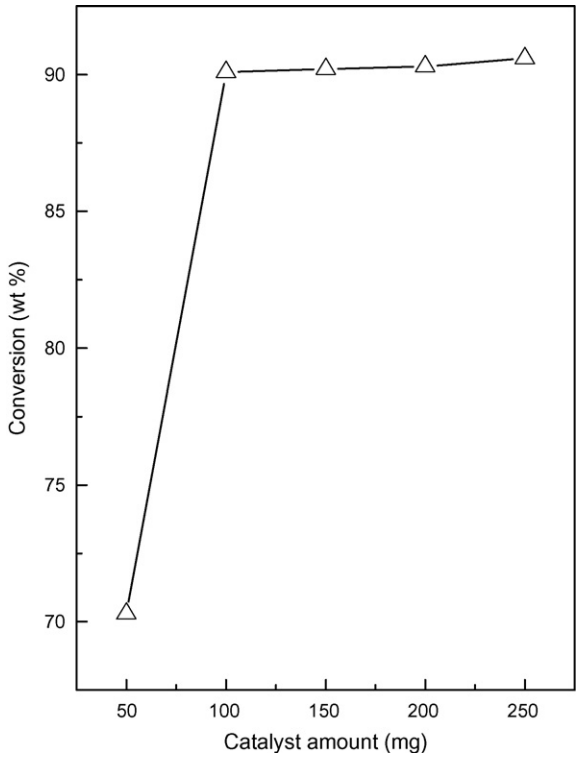

Fig. 11. Effect of catalyst weight on the esterification of 2-ethyl-1-hexanol with acetic acid in the presence of 35 wt% PWA/HZ catalyst in 5 h (molar ratio of alcohol/acid = 1:2, temperature 100 °C).

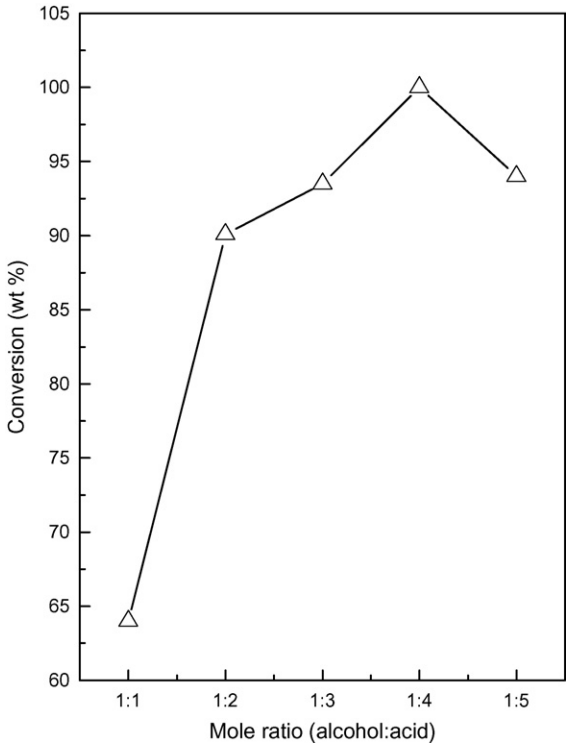

Fig. 13. wt% conversion of 2-ethyl-1-hexanol with different molar ratios of alcohol to acetic acid at 100 °C in the presence of 35 wt% PWA/HZ catalyst in 5 h (catalyst 0.1 g).

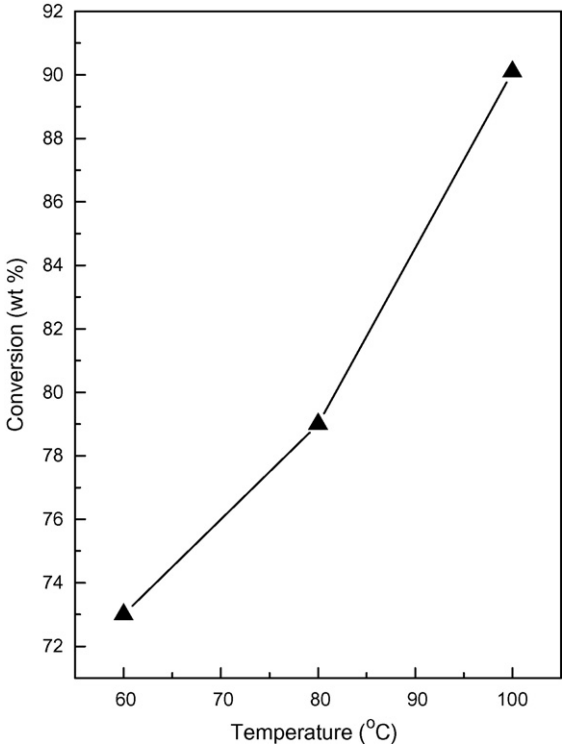

Fig. 12. wt% conversion of 2-ethyl-1-hexanol at different temperatures in the presence of 35 wt% PWA/HZ catalyst in 5 h (mole ratio of alcohol/acid = 1:2, catalyst 0.1 g).

is shown in Fig. 12. The results show that increasing temperature accelerates the forward reaction favouring the ester formation. The conversion of alcohol is ~17% higher for the experiment at 100 °C compared to the experiment at 60 °C.

3.8.5. *Influence of molar ratio of the reactants*

The molar ratio of alcohol to acid is an important factor which affects the yield of 2-ethyl-1-hexyl acetate ester. The effect of molar ratio of the reactants on the conversion of 2-ethyl-1-hexanol is shown in Fig. 13. Esterification of acetic acid with 2-ethyl-1-hexanol is an equilibrium-limited chemical reaction, and the use of excess 2-ethyl-1-hexanol increases the utilization of acetic acid. However, in the present study the less expensive acetic acid is taken in excess and esterification reactions have been carried out by varying the molar ratio of the reactants (alcohol to acid) between 1:2 and 1:5 using 35 wt% PWA/HZ catalyst. The reaction time is 5 h at 100 °C with catalyst weight kept constant at 0.10 g. The conversion of 2-ethyl-1-hexanol is found to increase rapidly from 64% with varying molar ratio of alcohol/acid from 1:1 to 1:5 reaching 100% at 1:4 ratio. So higher amounts of acid in the reaction mixture is suitable for obtaining high yield of ester on 35 wt% PWA/HZ catalyst at an optimum temperature of 100 °C in 5 h reaction time.

4. Conclusions

Unlike ZrO_2 and $Ce_xZr_{1-x}O_2$ supports, amorphous porous hydrous zirconia allows the growth of PWA crystallites. The PWA crystallites on hrdrous zirconia show characteristic IR bands while dispersed PWA on ZrO_2 and $Ce_xZr_{1-x}O_2$ supports show additional IR bands at 960 cm^{-1} and 1056 cm^{-1} [13,45]. The interaction of PWA with hydrous zirconia appears to be mainly through Zr–OH groups while on $Ce_xZr_{1-x}O_2$ the Keggin molecular ions are fixed to M^+ ions directly. PWA/HZ catalysts contain different acidic sites

which originate from hydroxyl groups of hydrous zirconia and dispersed PWA crystallites. The H_2-TPR behaviour of PWA crystallites dispersed on hydrous zirconia support depends on the interaction, amount PWA loaded and bulk like-nature of the crystallites. SEM and TEM analysis show the growth of ~7 nm size PWA crystallites for 35 wt% PWA dispersed on amorphous hydrous zirconia catalysts. PWA/HZ catalysts show good yields of 2-ethyl-1-hexyl acetate with 35 wt% loading of PWA at an optimum temperature of 100 °C in 5 h reaction time. The reaction involves proton transfer from catalyst to the adsorbed acid molecule which is further converted to ester by nucleophilic attack of hydroxyl group from the alcohol. The esterification of acetic acid with 2-ethyl-1-hexanol shows close to 90% conversion of 2-ethyl-1-hexanol with 100% selectivity towards 2-ethyl-1-hexyl acetate. The present catalytic system is easy to handle, non-corrosive and environmentally benign.

Acknowledgment

Financial support received from Defence Research and Development Organisation (DRDO), New Delhi, through Grant No. ERIP/ER/0300231/M/01/791 is gratefully acknowledged.

References

[1] Y. Ishii, K. Yamawaki, T. Ura, H. Yamada, T. Yoshida, M. Ogawa, J. Org. Chem. 53 (1988) 3587.
[2] I.A. Weinstock, E.M.G. Barbuzzi, M.W. Wemple, J.J. Cowan, R.S. Reiner, D.M. Sonnen, R.A. Heintz, J.S. Bond, C.L. Hill, Nature 414 (2001) 191.
[3] L.R. Pizzio, M.N. Blanco, Appl. Catal. A: Gen. 255 (2003) 265.
[4] A. Engin, H. Haluk, K. Gurkan, Green Chem. 5 (2003) 460.
[5] S. Patel, N. Purohit, A. Patel, J. Mol. Catal. A: Chem. 192 (2003) 195.
[6] S. Shanmugam, B. Viswanathan, T.K. Varadarajan, J. Mol. Catal. A: Chem. 223 (2004) 143.
[7] P. Sharma, S. Vyas, A. Patel, J. Mol. Catal. A: Chem. 214 (2004) 281.
[8] F.-M. Zhang, J. Wang, C.-S. Yuan, X.-Q. Ren, Catal. Lett. 102 (2005) 171.
[9] L. Yang, Y. Qi, X. Yuan, J. Shen, J. Kim, J. Mol. Catal. A: Chem. 229 (2005) 199.
[10] J.H. Sepúlveda, J.C. Yori, C.R. Vera, Appl. Catal. A: Gen. 288 (2005) 18.
[11] J. Das, K.M. Parida, J. Mol. Catal. A: Chem. 264 (2007) 248.
[12] K.M. Parida, S. Mallick, J. Mol. Catal. A: Chem. 275 (2007) 77.
[13] G. Ranga Rao, T. Rajkumar, Catal. Lett. 120 (2008) 261.
[14] A.D. Newman, D.R. Brown, P. Siril, A.F. Lee, K. Wilson, Phys. Chem. Chem. Phys. 8 (2006) 2893.
[15] D.P. Sawant, M. Hartmann, S.B. Halligudi, Micropor. Mesopor. Mater. 102 (2007) 223.
[16] P.M. Rao, A. Wolfson, S. Kababya, S. Vega, M.V. Landau, J. Catal. 232 (2005) 210.
[17] H.-Y. Shen, Z.M.A. Judeh, C.B. Ching, Q.-H. Xia, J. Mol. Catal. A: Chem. 212 (2004) 301.
[18] R. Neumann, M. Cohen, Angew. Chem. Int. Ed. Engl. 36 (1997) 1738.
[19] N. Bhatt, A. Patel, P. Selvam, K. Sidhpuria, J. Mol. Catal. A: Chem. 275 (2007) 14.
[20] N. Bhatt, C. Shah, A. Patel, Catal. Lett. 117 (2007) 146.
[21] M.G. Kulkarni, R. Gopinath, L.C. Meher, A.K. Dalai, Green Chem. 8 (2006) 1056.
[22] C. Huang, Z. Tang, Z. Zhang, J. Am. Ceram. Soc. 84 (2001) 1637.
[23] B.M. Devassy, F. Lefebvre, S.B. Halligudi, J. Catal. 231 (2005) 1.
[24] S. Mallik, K.M. Parida, S.S. Dash, J. Mol. Catal. A: Chem. 261 (2007) 172.
[25] E. López-Salinas, J.G. Hernández-Cortéz, I. Schifter, E. Torres-García, J. Navarrete, A. Gutiérrez-Carrillo, T. López, P.P. Lottici, D. Bersani, Appl. Catal. A: Gen. 193 (2000) 215.
[26] F.G.R. Gimblett, A.A. Rahman, K.S.W. Sing, J. Colloid Interface Sci. 102 (1984) 483.
[27] G.K. Chuah, S. Jaenicke, B.K. Pong, J. Catal. 175 (1998) 80.
[28] P. Afanasiev, A. Thiollier, M. Breysse, J.L. Dubois, Top. Catal. 8 (1999) 147.
[29] G.K. Chuah, S.H. Liu, S. Jaenicke, J. Li, Micropor. Mesopor. Mater. 39 (2000) 381.
[30] G. Aguila, S. Guerrero, F. Gracia, P. Araya, Appl. Catal. A: Gen. 305 (2006) 219.
[31] X. Qu, Y. Guo, C. Hu, J. Mol. Catal. A: Chem. 262 (2007) 128.
[32] W. Kuang, A. Rives, M. Fournier, R. Hubaut, Appl. Catal. A: Gen. 250 (2003) 221.
[33] T. López, R. Gómez, J.G. Hernández, E. López-Salinas, X. Bokhimi, A. Morales, J.L. Boldú, E. Muñoz, O. Novaro, Langmuir 15 (1999) 5820.
[34] C. Jiang, Y. Guo, C. Wang, C. Hu, Y. Wu, E. Wang, Appl. Catal. A: Gen. 256 (2003) 203.
[35] I.V. Kozhevnikov, K.R. Kloetstra, A. Sinnema, H.W. Zandbergen, H. van Bekkum, J. Mol. Catal. A: Chem. 114 (1996) 287.
[36] T. Chang, J. Chem. Soc. (Faraday Trans.) 91 (1995) 375.
[37] A. Ghanbari-Siahkali, A. Philippou, J. Dwyer, M.W. Anderson, Appl. Catal. A: Gen. 192 (2000) 57.
[38] N. Essayem, R. Frety, G. Coudurier, J.C. Vedrine, J. Chem. Soc. (Faraday Trans.) 93 (1997) 3243.
[39] G. Koyano, K. Ueno, M. Misono, Appl. Catal. A: Gen. 181 (1999) 267.
[40] M.E. Chimienti, L.R. Pizzio, C.V. Cáceres, M.N. Blanco, Appl. Catal. A: Gen. 208 (2001) 7.
[41] I.V. Kozhevnikov, J. Mol. Catal. A: Chem. 262 (2007) 86.
[42] C.L. Bianchi, V. Ragaini, C. Pirola, G. Carvoli, Appl. Catal. B: Environ. 40 (2003) 93.
[43] S. Ajaikumar, A. Pandurangan, J. Mol. Catal. A: Chem. 266 (2007) 1.
[44] V. Ragaini, C.L. Bianchi, C. Pirola, G. Carvoli, Appl. Catal. B: Environ. 64 (2006) 66.
[45] G. Ranga Rao, T. Rajkumar, J. Colloid Interface Sci. 324 (2008) 134.